Smart Structures and Systems, *Vol. 28, No. 6 (2021) 737-744*
https://doi.org/10.12989/sss.2021.28.6.737

Structural health monitoring of CFRPs using electrical resistance by reduced peripheral electrodes

Young-Bin Park*[2], Hyung Doh Roh [1a] and In Yong Lee [2b]

[1] *Composites Research Division, Korea Institute of Materials Science, Changwon-daero 797, Changwon, Gyeongnam 51508, Republic of Korea*
[2] *Department of Mechanical Engineering, Ulsan National Institute of Science and Technology, UNIST-gil 50, Ulju-gun, Ulsan 44919, Republic of Korea*

(*Received February 26, 2021, Revised June 22, 2021, Accepted August 6, 2021*)

Abstract. In this study, structural health monitoring (SHM) methods of carbon fiber reinforced plastics (CFRPs) were investigated using electrical resistance. The developed sensing technique monitored electrical resistance in accordance with the impact damage of a CFRP. The changes in electrical resistances with multiple electrode sets enabled SHM without extra sensors so that this technique can be called self-sensing. Moreover, this study proposed electrodes only at peripheral side of a structure to minimize the number of electrodes compared to those in an array which has square number of sensors as the sensing area increases. For the intensive investigation, electromechanical sensitivity in terms of electrode distance was analyzed and optimized under drop weight impact testing. Then, SHM methods with electrodes in an array and electrodes in peripheral edges were comparatively investigated. The developed methods successfully localized impact damages into 2D coordinates. Furthermore, damage severity can be shown with a damage map by calculating electrical resistance change ratio. Therefore, structural health self-sensing system using electrical resistance was successfully developed with the minimum number of electrodes.

Keywords: carbon fiber reinforced polymer; composites; nondestructive evaluation; smart materials; structural health monitoring (SHM)

1. Introduction

The needs for structural health monitoring (SHM) of a carbon fiber reinforced plastic (CFRP) has been increased, because the structural safety of a CFRP is directly involved in maintenance cost and casualties (Karayannis *et al*. 2015, Carboni *et al*. 2015, Ghodrati *et al*. 2011). Especially, monitoring for impact damage is getting spotlights in applications of vehicles (Cocchi *et al*. 2020, Vertuccio *et al*. 2020), aircrafts (Gohardani *et al*. 2014, Wang *et al*. 2018) and civil infrastructures (Casciati *et al*. 2016, Yu *et al*. 2010).

SHM of CFRP consists of schedule-based monitoring and condition-based monitoring. Schedule-based monitoring investigates structural health periodically. The examples of the schedule-based are eddy current (He *et al*. 2014a, b, Liang *et al*. 2016, Mizukami *et al*. 2016) and C-scan (Suvarna *et al*. 2014, Post *et al*. 2017, Hauffe *et al*. 2020). The schedule-based monitoring techniques are usually utilized to scan the overall structures when the structures are not in-service. However, the condition-based monitoring detects change in structural condition even when the structures are working. The examples of the condition-based are fiber Bragg grating (Geng *et al*. 2017, Ju *et al*. 2018, Lu *et al*. 2015), strain gauge (Cho *et al*. 2010) and PZT (Kim *et al*. 2012, and Zhong and Xiang 2019). While the condition-based monitoring techniques hold advantages in real-time monitoring, the detecting area of a sensor is limited so that the sensing elements should be installed in an array. Therefore, the studies for detecting the whole structure with the minimum number of sensors have been required.

Self-sensing of CFRP was investigated by numerous researchers (Kalashnyk *et al*. 2017, Gallo and Thostenson 2015, Kwo *et al*. 2016). The word 'self-sensing' refers to detecting structural health using changes in structural condition without extra sensors. In this field, electrical resistance of carbon fiber network was commonly analyzed to investigate structural health of CFRPs. D.D.L. Chung group (Wang and Chung 2013, Xi and Chung 2019, Ramirez and Chung 2016, Chung 2016, Wang and Chung 2006) investigated analyzed self-sensing capability of CFRPs in various electrode pairings by flexural testing. They verified that electrode pairings at the same plane represented less noise in electrical resistance changes. Plus, they concluded that the magnitude of electrical resistance change was related to the maximum deflection of a CFRP, and hence, deflection self-sensing was available by monitoring electrical resistance of a CFRP. However, their results were not extended to the large-scale monitoring with

*Corresponding author, Professor,
E-mail: ypark@unist.ac.kr
[a] Ph.D., E-mail: hdroh@kims.re.kr
[b] Ph.D. Student, E-mail: number1dog@unist.ac.kr

ISSN: 1738-1584 (Print), 1738-1991 (Online)

multiple sets of electrodes, but single section with multiple electrode pairings.

A. Todoroki group investigated electromechanical behavior of uni-directional CFRP in elastic region (Todoroki *et al*. 2009, 2014). They correlated classic laminate plate theory and electrical resistance change from multi-axial static tensile loading. Moreover, they developed self-sensing methods for delamination by analyzing electrical resistance (Todoroki *et al*. 2015, Todoroki 2014, Yamane and Todoroki 2016). While the studies of A. Todoroki group investigated multi-directional electromechanical behavior, their detecting areas were limited to the single electrode pairing unit similar to other results.

Naghashpour and Hoa (2013, 2014, 2017) studied impact self-sensing using carbon nanotubes (CNTs). They made a glass fiber reinforced plastic with CNTs, and analyzed the dispersion of CNTs using electrical resistance. For the impact self-sensing, electrodes were installed in an array, for example, 50 electrodes were required to divide a testing CFRP into 25 cells. The originality of this research compared to previous studies underlies in the sensing area with multiple sensing units. The damage localization performance was limited to the cell size, which was a distance between two electrodes. These limitations were also observed in other studies (Vaidya and Allouche 2011). However, the number of electrodes were squared as the size of the structure became larger. Therefore, the study for the minimized electrodes with larger detecting area has been steadily required.

From the literature review, studies for impact self-sensing of CFRPs without extra sensors in SHM fields were quite limited. Therefore, this study investigated the impact self-sensing using electrical resistance to not only enhance the sensing performance but also reduce the number of electrodes of CFRPs.

2. Experimental

2.1 Materials

3K plain-woven carbon fiber (Mitsubishi, Japan) with a ply thickness of approximately 0.2 mm and a density of 199 g/m^2 was supplied by JMC (Gyeongju, Korea). The carbon fiber bundle, which is called 3K carbon fiber, consisted of 3000 carbon fiber filaments. The plain-woven indicates the weaving type of the fabric. The warp and the weft were woven perpendicularly with the same amounts of bundles. In specific, the 3K carbon fiber bundle were perpendicularly woven into a fabric. The polymer matrix used was vinylester resin (RF-1001MV, Cray Valley Korea), and it consisted of 45% styrene and 55% epoxy acrylate. The curing agent was methyl ethyl ketone peroxide, manufactured by Arkema, and the mixing ratio was 1 wt% of the matrix. Both the polymer matrix and the curing agent were supplied by Jet Korea Corp. (Changwon, Korea).

2.2 Sample preparation

The dimension of the carbon fiber was 300 mm × 300 mm, and four or eight plies of carbon fiber were stacked. Copper wires (30 AWG) were embedded into the topmost ply of the dry carbon fiber using a silver paste (Elcoat P-100, CANS, Japan) to minimize the contact resistance. Composite fabrication was performed by vacuum-assisted resin transfer molding (VARTM), and epoxy adhesive (Araldite, USA) was used to firmly fix the electrodes.

A rectangular CFRP for the sensitivity optimization was manufactured with a geometry of 300 and 100 mm as shown in Fig. 1(a). Eight electrodes were aligned and installed along the length. The distance of electrode pairs which are indicated in the same color in red, yellow, green and blue in Fig. 1(a) were 60, 120, 180, and 240 mm, respectively.

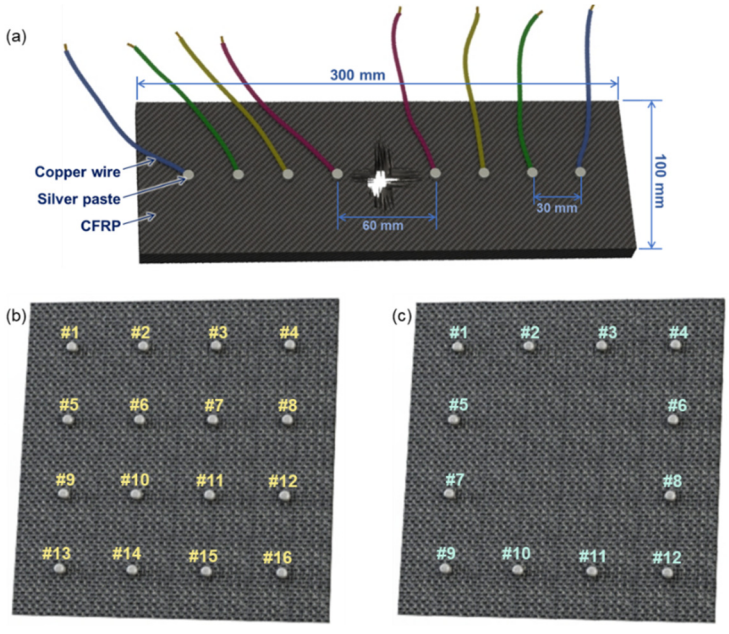

Fig. 1 (a) Geometry and electrode placement of a CFRP for sensitivity analysis, Schematics of CFRPs of (b) “array type” and (c) “periphery type”

A CFRP, which has electrodes installed in an array as shown in Fig. 1(b), was named "array type." The electrode configuration of the array type might be 3 × 3, 4 × 4, or 5 × 5, and the distances between adjacent electrodes were 100, 80, and 60 mm, respectively. Another CFRP, which had electrodes in periphery, was named "periphery type." For example, 4 by 4 periphery CFRP had 12 electrodes at four edges as shown in Fig. 1(c).

2.3 Characterization

Drop weight impact tester (CEAST 9350, INSTRON, USA) was employed at the room temperature to generate the impact energy for CFRPs. The CFRP samples were fixed by a pneumatic 40-mm-diameter circular clamp with a clamping force of 40 N.

A multimeter (Keithley 2002, USA) and switching system (Keithley 7001, USA) were used to measure the electrical resistance variations during the impact tests at a sampling rate of 9.4 plots per second. The analysis method for damage localization was developed considering the ratio of the electrical resistance variation using the numerical computing software MATLAB. Additionally, a damage visualized map was also plotted with the analysis of damage localization. Moreover, LED matrix was utilized to visualize damage location and its severity connected with Arduino. The changes in electrical resistance were measured by the multimeter, and then the software and Arduino make the LED matrix emitted in accordance with the resistance changes.

2.4 Finite element analysis

The commercially released FEA software, ABAQUS, was employed to investigate the electrical variations of CFRPs in 3D. The inherent principle of the FEA is represented by Maxwell's partial differential equation (PDE) in terms of electrical current flow.

The purpose of the FEM is to rationalize the electrical model of a CFRP. FEM with PDE solved electrical current density in the CFRP, and electrical resistance was additionally calculated to analyze the resistance changes in terms of the impact damage. Then, this result was comparatively investigated with empirical data in order to validate the proposed electrical model.

The FEA model of a CFRP comprised four homogeneous layers with a thickness of 0.2 mm each, and three plies of homogeneous layers with a thickness of 0.05 mm each, between the aforementioned layers, as a fiber-overlapped area in the CFRP. Punctured area was simplified into 12-mm-diameter hole. Delamination was realized around the hole by extracting the fiber-overlapped area. The delamination had a 14-mm outer-diameter and 12-mm inner-diameter. The electrical conductivity of the CFRP layer was set as 29 S/m and that of the fiber-overlapped area at 43.5 S/m. In addition, the conductivity of the electrode was set to 10^{36} S/m so that input potential of 1 and 0 V could be imposed on the electrodes without resistance.

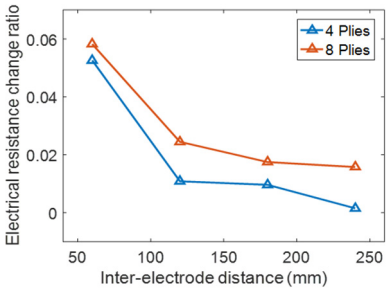

Fig. 2 Electromechanical sensitivity of CFRPs as a function of the inter-electrode distance

3. Results and discussion

3.1 Electromechanical sensitivity analysis

A drop weight impact tester hit the center of the rectangular CFRP, resulting in a puncture. The consequent electrical resistance variation ratios are represented in Fig. 2. Most of the electrical resistance values increased because the middle sections of the electrical paths underwent detours due to the puncture. The increment of the resistance variation decreased as the distance between the electrodes increased, regardless of the number of carbon fiber plies in the CFRP.

3.2 Self-sensing in an array type

In-situ self-sensing algorithm was developed, and applied to an array-form to realize real-time CFRP SHM. The algorithm analyzed the electrical resistance changes of array cells for the damage localization. The electrical resistances between the adjacent electrodes were measured, and the resistance variation ratios were represented as a bar graph in an array, as shown in Fig. 3(a). The array was visualized and re-mapped into a damage map, as demonstrated in Fig. 3(b).

Electromechanical behavior of CFRPs with respect to the impact damage is shown in Fig. 4. Impact damage localization has been successful in the regions indicated by magenta circles. The coordinates of the impacted spot represented the highest peak in the visualized damage maps which has the same coordinates with the magenta circles. Yellow color in the map represents the largest electrical resistance variation, whereas the blue color indicates slight variations in the electrical resistance. The drop-weight-impacted spot endured the largest electrical resistance variation, regardless of the input energy. Further, the damage map was representative of the electrical resistance variations of the adjacent channels, and this information enhanced the sensing performance. Therefore, damage localization was attained by monitoring the resistance variations of the multiple channels.

Analysis of electromechanical sensitivity in terms of inter-electrode distance that was introduced in Fig. 1(a) has been extended into a 2D array as shown in Fig. 5. Additionally, damage localization for different inter-electrode distances was also successful. The largest

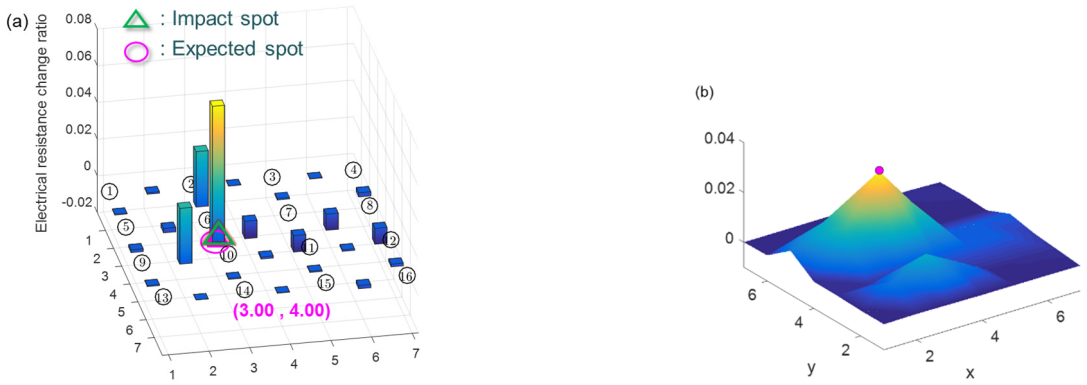

Fig. 3 Electromechanical analysis of an array-type sample: (a) electrode configuration and electrical resistance change ratio; and (b) a visualized damage map

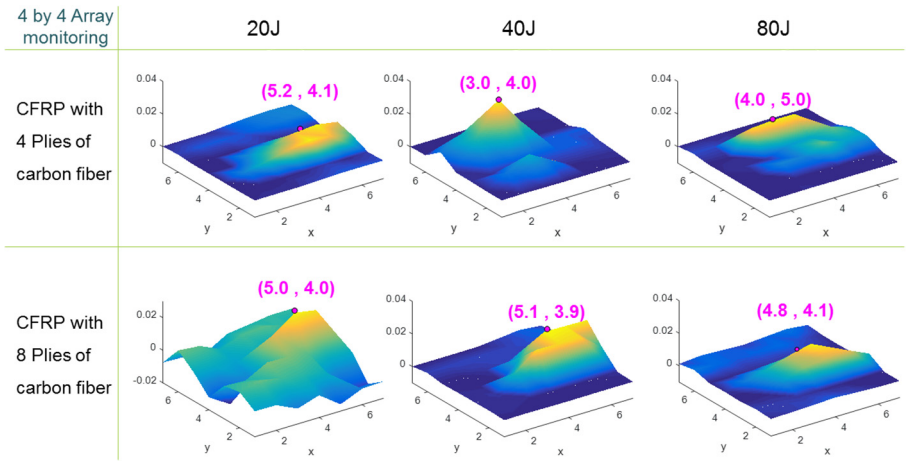

Fig. 4 Visualized damage maps of 4-ply- and 8-ply-CFRPs for different impact energy values

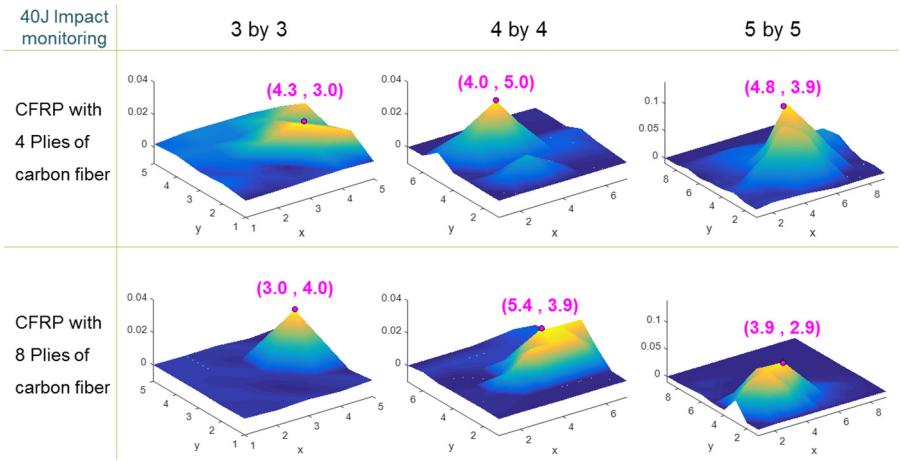

Fig. 5 Visualized damage maps of 4-ply- and 8-ply-CFRPs for different electrode arrangements

resistance variations were observed at the impacted area, whereas the slight resistance variations were monitored when the impact location was further from the measuring electrode pair. The resistance variations nearby were also utilized for more accurate damage localization.

Electromechanical sensitivities of CFRPs decreased when the distance between the adjacent electrodes increased, as shown in Fig. 6. Inter-electrode distances of 3 × 3, 4 × 4, and 5 × 5 CFRPs were 55, 75, and 110 mm, respectively. The volumetric change ratio of mechanical failure compared with the original volume between the electrodes was related to the electrical resistance variation ratio, such that the 5 × 5 CFRP, with the inter-electrode distance of 55 mm, represented the largest electrical resistance variations.

The accuracy of impact damage localization was

Table 1 Error analysis of impact damage localization

Samples	Measured X coordinate	Measured Y coordinate	Actual X coordinate	Actual Y coordinate	Distance (cell)	Localizing error (mm)
A	5.19	4.12	5	4	0.22	8.41
B	3.00	4.00	3.00	4.00	0.00	0.00
C	4.00	5.00	4.00	5.00	0.00	0.00
D	4.25	3.00	4.00	3.00	0.25	14.06
E	4.77	3.92	5.00	4.00	0.24	6.84
F	5.00	4.00	5.00	4.00	0.00	0.00
G	5.08	3.92	5.00	4.00	0.12	4.42
H	4.81	4.12	5.00	4.00	0.22	8.41
I	3.00	4.00	3.00	4.00	0.00	0.00
J	3.91	2.91	4.00	3.00	0.13	3.62

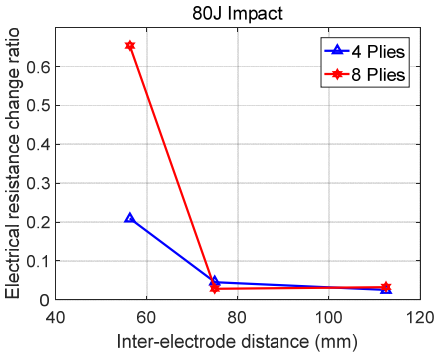

Fig. 6 Electromechanical sensitivities of CFRPs as a function of the inter-electrode distance

analyzed, as shown in Table 1. The average error of a sensing array was approximately 6% of an array cell that was 6% of the inter-electrode distance, and the average error in the metric scale was 4.58 mm. This result can facilitate optimizing the sensing performance by modifying the error and sensitivity values that are acquired from Figs. 2(b) and 6.

3.3 Self-sensing with electrodes at the periphery

Electromechanical behaviors and damage localizing procedures of CFRPs with electrodes at the periphery are shown in Fig. 7. The decision-making procedures for the damage localization with different number of electrodes resulted in some differences. When the number of electrodes on one side is odd, the procedure of damage localizing might be similar to that of the 3 × 3 periphery CFRP, shown in Fig. 7. The arrows in sky-blue in Fig. 7 indicate the directions of measuring the electrical channel. When the number of electrodes is even, it is similar to the 4 × 4 periphery CFRP. The inherent algorithms for the damage localization is based on the summation of electrical resistance variation of the adjacent channels. Moreover, posing the weighing factor of 10 into the largest changed channels, the mid-points of electrical channels were standardized into 2D coordinates. Then, damage loczliza-

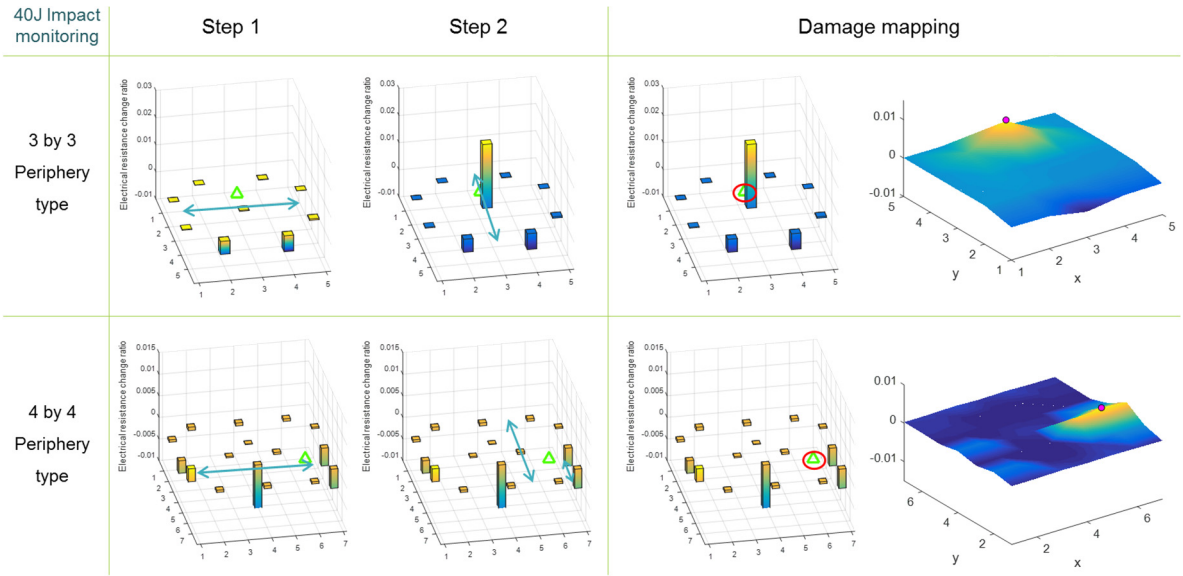

Fig. 7 Decision-making procedure of damage localization with electrodes at the periphery

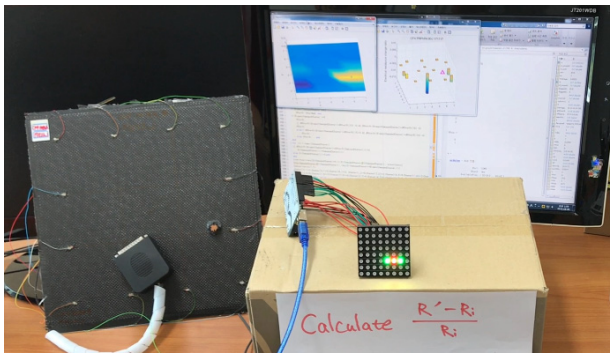

Fig. 8 Potential application of the proposed damage localization using Arduino and LEDs

tion was successfully demonstrated in a colormap.

Self-sensing SHM algorithm is applicable to a schedule-based system as well as a real-time monitoring system. The potential application of the SHM system was conformed with Arduino and LED matrix, as shown in Fig. 8. The CFRP underwent electrical network changes by impact damages, and the multimeter acquired the changes in electrical resistance. Then, the LED matrix connected to Arduino demonstrated the resistance changes.

Both damage localization and damage severity are indicated in red and green lights, respectively. If the monitoring system observes the resistance variation in real-time, the system can be real-time-monitored by SHM. However, if the resistance analysis is performed periodically, the system can be schedule-based monitored by SHM. In the schedule-based system, the resistance values can be extracted with a one-touch coupler and a multimeter without any sensing element.

3.4 FEA for electrical resistance analysis

The model for electrical resistivity analysis of a CFRP was proposed, as shown in Fig. 9(a). The CFRP model had overlapped zones between the carbon fiber laminae, called the inter-ply area. The rationale for the overlapped area was based on the empirical data that is represented in Fig. 9(b). Both the measured resistivity and the laminar-thickness decreased as the number of carbon fiber plies increased from two to eight. Numerical analysis results of the proposed model agreed well with the empirical data, as shown in Fig. 9(b).

Fig. 10 shows the 3D FEA result of the CFRP model illustrated in Fig. 9. Electrical current density in the center of the CFRP was changed due to the formation of the

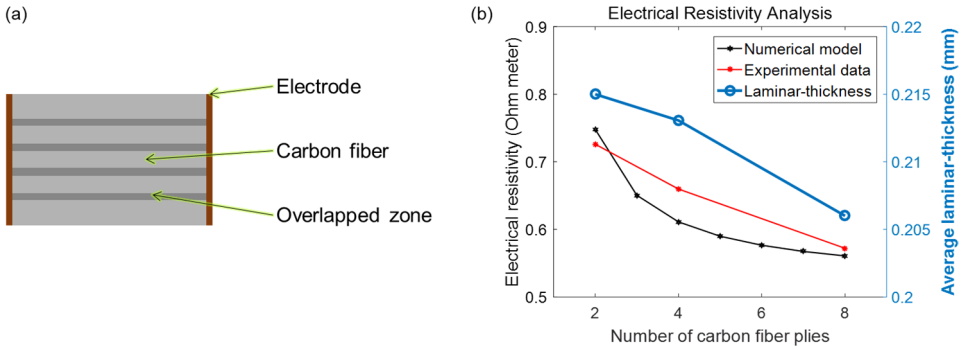

Fig. 9 (a) Cross-sectional schematic of the proposed CFRP model; (b) Electrical resistivity as a function of the number of carbon fiber plies

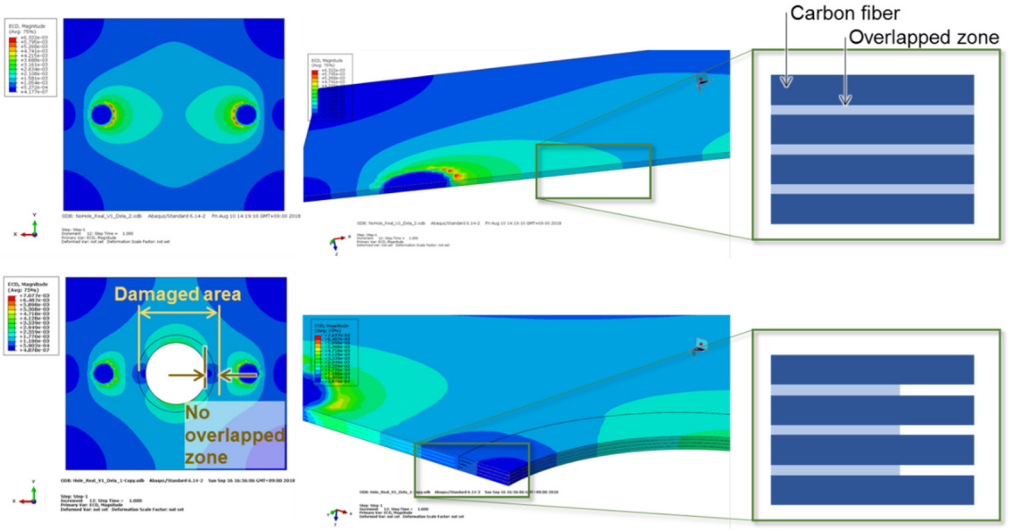

Fig. 10 Electrical current density analyzed by FEA based on the proposed model

impact damage at the center. Electrical current density was concentrated in the horizontal line connecting the two electrodes. However, the current density was focused on the upper and lower sides of the damaged spot because electrons prefer the easiest path between two electrodes.

Electrical resistance must be increased with impact damage of the CFRP because the electrical current density underwent variations in the dominant path along the arc of the puncture. Moreover, delamination near the impact spot caused the elimination of the inter-ply area, for which the electrical conductivity was found to be higher than a general carbon fiber, shown in Fig. 9. The measured electrical resistance of the FEA model, represented in Fig. 10, was changed from 4.65 to 6.02 Ω.

4. Conclusions

In this study, electromechanical behavior of a CFRP was investigated by drop weight impact testing. The electrical resistance changed due to the impact damage because of the alteration in the electrically conductive carbon fiber network. The volumetric change ratio at the periphery of an electrode set with respect to the location of the puncture, affected the electrical resistance variation ratio. In other words, the distance between electrodes were involved in electromechanical sensitivity. The smaller electrode distance showed the larger resistance change accompanied by the larger structural change ratio. Therefore, the inter-electrode distance was analyzed to optimize the self-sensing sensitivity for SHM.

SHM using electrical resistance was extended to larger CFRPs with electrodes in an array. The largest electrical resistance variation ratio indicated the impact spot using array-type bar graphs and damage maps. Moreover, SHM was performed with electrodes only at the periphery. Decision-making algorithms for the periphery type were suggested using summations of the adjacent electrical channels with different weight factors. The error of damage localization was approximately 4.6 mm. Therefore, the CFRP self-sensing system with a smaller number of electrodes was developed for SHM.

Periphery type was additionally investigated for self-sensing with lesser number of electrodes. Electrodes only at the periphery were used to localize the impact damage. Decision-making algorithm for damage localization was also developed, depending on the number of electrodes at one side.

A novel CFRP electrical model was developed for the FEA of electrical current density. The FEA supported the fundamental principle of self-sensing based on the electrical resistance values. A hole generated from the impact puncture, not only changed the dominant electrical path, but also the electrical resistance. Therefore, analyzing the electrical path via electrically conductive carbon fiber facilitated the understanding of the self-sensing mechanism of a CFRP.

Acknowledgments

This work was supported by the National Research Foundation of Korea (NRF) grant funded by the Ministry of Science and ICT, Korea (NRF-2017R1A5A1015311).

References

Andreades, C., Fierro, G.P.M. and Meo, M. (2020), "A nonlinear ultrasonic SHM method for impact damage localisation in composite panels using a sparse array of piezoelectric PZT transducers", *Ultrasonics*, **108**, 106181. https://doi.org/10.1016/j.ultras.2020.106181

Carboni, M., Gianneo, A. and Giglio, M. (2015), "A Lamb waves based statistical approach to structural health monitoring of carbon fibre reinforced polymer composites", *Ultrasonics*, **60**, 51-64. https://doi.org/10.1016/j.ultras.2015.02.011

Casciati, S, Chen, Z.C., Faravelli, L. and Vece, M. (2016), "Synergy of monitoring and security", *Smart Struct. Syst., Int. J.*, **17**(5), 743-751. https://doi.org/10.12989/sss.2016.17.5.743

Cho, S., Jo, H., Jang, S., Park, J., Yun, C.-B. and Seo, J.-W. (2010), "Structural health monitoring of a cable-stayed bridge using wireless smart sensor technology: data analyses", *Smart Struct. Syst., Int. J.*, **6**(5-6), 461-480. https://doi.org/10.12989/sss.2010.6.5_6.461

Chung, D.D.L. (2016), *Advanced Composite Materials for Aerospace Engineering*, edited by S. Rana and R. Fangueiro, Woodhead Publishing, pp. 295-331.

Cocchi, D., Raimondi, L., Brugo, T.M. and Zucchelli, A. (2020), "A systematic material-oriented design approach for lightweight components and the CFRP motor wheel case study", *Int. J. Adv. Manuf. Technol.*, **109**(7), 2133-2153. https://doi.org/10.1007/s00170-020-05756-2

Gallo, G.J. and Thostenson, E.T. (2015), "Electrical characterization and modeling of carbon nanotube and carbon fiber self-sensing composites for enhanced sensing of microcracks", *Mater. Today Commun.*, **3**, 17-26. https://doi.org/10.1016/j.mtcomm.2015.01.009

Geng, X., Jiang, M., Gao, L., Wang, Q., Jia, Y., Sui, Q., Jia, L. and Li, D. (2017), "Sensing characteristics of FBG sensor embedded in CFRP laminate", *Measurement*, **98**, 199-204. https://doi.org/10.1016/j.measurement.2016.12.003

Ghodrati, A.G., Seyed, R.S.A. and Bagheri, A. (2011), "Damage detection in plates based on pattern search and Genetic algorithms", *Smart Struct. Syst., Int. J.*, **7**(2), 117-132. http://doi.org/10.12989/sss.2011.7.2.117

Gohardani, O., Elola, M.C. and Elizetxea, C. (2014), "Potential and prospective implementation of carbon nanotubes on next generation aircraft and space vehicles: A review of current and expected applications in aerospace sciences", *Progress Aerosp. Sci.*, **70**, 42-68. https://doi.org/10.1016/j.paerosci.2014.05.002

Hauffe, A., Hähnel, F. and Wolf, K. (2020), "Comparison of algorithms to quantify the damaged area in CFRP ultrasonic scans", *Compos. Struct.*, **235**, 111791. https://doi.org/10.1016/j.compstruct.2019.111791

He, Y., Tian, G., Pan, M. and Chen, D. (2014a), "Impact evaluation in carbon fiber reinforced plastic (CFRP) laminates using eddy current pulsed thermography", *Compos. Struct.*, **109**, 1-7. https://doi.org/10.1016/j.compstruct.2013.10.049

He, Y., Tian, G., Pan, M. and Chen, D. (2014b), "Non-destructive testing of low-energy impact in CFRP laminates and interior defects in honeycomb sandwich using scanning pulsed eddy current", *Compos. Part B: Eng.*, **59**, 196-203. https://doi.org/10.1016/j.compositesb.2013.12.005

Ju, M., Park, K., Moon, D. and Park, C. (2018), and Sim, J., "On

strain measurement of smart GFRP bars with built-in fiber Bragg grating sensor", *Smart Struct. Syst.*, *Int. J.*, **65**(2), 155-162. http://doi.org/10.12989/sem.2018.65.2.155

Kalashnyk, N., Faulques, E., Schjødt-Thomsen, J., Jensen, L.R., Rauhe, J.C.M. and Pyrz, R. (2017), "Monitoring self-sensing damage of multiple carbon fiber composites using piezoresistivity", *Synthetic Metals*, **224**, 56-62. https://doi.org/10.1016/j.synthmet.2016.12.021

Karayannis, C.G., Voutetaki, M.E., Chalioris, C.E., Providakis, C.P. and Angeli, G.M. (2015), "Detection of flexural damage stages for RC beams using piezoelectric sensors (PZT)", *Smart Struct. Syst.*, *Int. J.*, **15**(4), 997-1018. http://doi.org/10.12989/sss.2015.15.4.997

Kim, J.-W., Lee, C. and Park, S. (2012), "Damage Localization for CFRP-Debonding Defects Using Piezoelectric SHM Techniques", *Res. Nondestruct. Eval.*, **23**(4), 183-196. http://dx.doi.org/10.1080/09349847.2012.660244

Kwon, D.-J., Shin, P.-S., Kim, J.-H., Wang, Z.-J., DeVries, K.L. and Park, J.-M. (2016), "Detection of damage in cylindrical parts of carbon fiber/epoxy composites using electrical resistance (ER) measurements", *Compos. Part B: Eng.*, 99, 528-532. https://doi.org/10.1016/j.compositesb.2016.06.050

Liang, T., Ren, W., Tian, G.Y., Elradi, M. and Gao, Y. (2016), "Low energy impact damage detection in CFRP using eddy current pulsed thermography", *Compos. Struct.*, **143**, 352-361. https://doi.org/10.1016/j.compstruct.2016.02.039

Lu, S., Jiang, M., Sui, Q., Sai, Y. and Jia, L. (2015), "Low velocity impact localization system of CFRP using fiber Bragg grating sensors", *Optical Fiber Technol.*, **21**, 13-19. https://doi.org/10.1016/j.yofte.2014.07.003

Mizukami, K., Mizutani, Y., Kimura, K., Sato, A., Todoroki, A. and Suzuki, Y. (2016), "Detection of in-plane fiber waviness in cross-ply CFRP laminates using layer selectable eddy current method", *Compos. Part A: Appl. Sci. Manuf.*, **82**, 108-118. https://doi.org/10.1016/j.compositesa.2015.11.040

Naghashpour, A. and Van Hoa, S. (2013), "A technique for real-time detection, location and quantification of damage in large polymer composite structures made of electrically non-conductive fibers and carbon nanotube networks", *Nanotechnology*, **24**(45), 455502. https://doi.org/10.1088/0957-4484/24/45/455502

Naghashpour, A. and Van Hoa, S. (2014), "A technique for real-time detecting, locating, and quantifying damage in large polymer composite structures made of carbon fibers and carbon nanotube networks", *Struct. Health Monitor.*, **14**(1), 35-45. https://10.1177/1475921714546063

Naghashpour, A. and Van Hoa, S. (2017), "Requirements of amount of carbon nanotubes for damage detection in large polymer composite structures", *Polym. Testing*, **63**, 407-416. https://doi.org/10.1016/j.polymertesting.2017.08.013

Post, W., Kersemans, M., Solodov, I., Van Den Abeele, K., García, S.J. and van der Zwaag, S. (2017), "Non-destructive monitoring of delamination healing of a CFRP composite with a thermoplastic ionomer interlayer", *Compos. Part A: Appl. Sci. Manuf.*, **101**, 243-253. https://doi.org/10.1016/j.compositesa.2017.06.018

Ramirez, M. and Chung, D.D.L. (2016), "Electromechanical, self-sensing and viscoelastic behavior of carbon fiber tows", *Carbon*, **110**, 8-16. https://doi.org/10.1016/j.carbon.2016.08.095

Suvarna, R., Arumugam, V., Bull, D.J., Chambers, A.R. and Santulli, C. (2014), "Effect of temperature on low velocity impact damage and post-impact flexural strength of CFRP assessed using ultrasonic C-scan and micro-focus computed tomography", *Compos. Part B: Eng.*, **66**, 58-64. https://doi.org/10.1016/j.compositesb.2014.04.028

Todoroki, A. (2014), "Monitoring of electric conductance and delamination of CFRP using multiple electric potential measurements", *Adv. Compos. Mater.*, **23**(2), 179-193. http://doi.org/10.1080/09243046.2013.844900

Todoroki, A., Samejima, Y., Hirano, Y. and Matsuzaki, R. (2009), "Piezoresistivity of unidirectional carbon/epoxy composites for multiaxial loading", *Compos. Sci. Technol.*, **69**(11), 1841-1846. https://doi.org/10.1016/j.compscitech.2009.03.023

Todoroki, A., Haruyama, D., Mizutani, Y., Suzuki, Y. and Yasuoka, T. (2014), "Electrical resistance change of carbon/epoxy composite laminates under cyclic loading under damage initiation limit", *Open J. Compos. Mater.*, **4**(1). http://doi.org/10.10.4236/ojcm.2014.41003

Todoroki, A., Yamada, K., Mizutani, Y., Suzuki, Y. and Matsuzaki, R. (2015), "Impact damage detection of a carbon-fibre-reinforced-polymer plate employing self-sensing time-domain reflectometry", *Compos. Struct.*, **130**, 174-179. https://doi.org/10.1016/j.compstruct.2015.04.020

Vaidya, S. and Allouche, E.N. (2011), "Experimental evaluation of electrical conductivity of carbon fiber reinforced fly-ash based geopolymer", *Smart Struct. Syst.*, *Int. J.*, **7**(1), 27-40. http://doi.org/10.12989/sss.2011.7.1.027

Vertuccio, L., Spinelli, G., Lamberti, P., Tucci, V., Zarrelli, M., Russo, S., Iannuzzo, G. and Guadagno, L. (2020), "Self-sensing nanocomposites in automotive/aeronautic field", *Mater. Today: Proceedings*, **34**, 125-127. https://doi.org/10.1016/j.matpr.2020.01.409

Wang, S. and Chung, D.D.L. (2006), "Self-sensing of flexural strain and damage in carbon fiber polymer-matrix composite by electrical resistance measurement", *Carbon*, **44**(13), 2739-2751. https://doi.org/10.1016/j.carbon.2006.03.034

Wang, D. and Chung, D.D.L. (2013), "Through-thickness piezoresistivity in a carbon fiber polymer-matrix structural composite for electrical-resistance-based through-thickness strain sensing", *Carbon*, **60**, 129-138. https://doi.org/10.1016/j.carbon.2013.04.005

Wang, Z., Qiao, P. and Shi, B. (2018), "Effective time-frequency characterization of Lamb wave dispersion in plate-like structures with non-reflecting boundaries", *Smart Struct. Syst.*, *Int. J.*, **21**(2), 195-205. https://doi.org/10.12989/sss.2018.21.2.195

Xi, X. and Chung, D.D.L. (2019), "Piezoelectric and piezoresistive behavior of unmodified carbon fiber", *Carbon*, **145**, 452-461. https://doi.org/10.1016/j.carbon.2019.01.044

Yamane, T. and Todoroki, A. (2016), "Electric potential function of oblique current in laminated carbon fiber reinforced polymer composite beam", *Compos. Struct.*, **148**, 74-84. https://doi.org/10.1016/j.compstruct.2016.03.047

Yu, Y., Ou, J. and Li, H. (2010), "Design, calibration and application of wireless sensors for structural global and local monitoring of civil infrastructures", *Smart Struct. Syst.*, *Int. J.*, **6**(5-6), 641-659. https://doi.org/10.12989/sss.2010.6.5_6.641

Zhong, Y. and Xiang, J. (2019), "Impact location on a stiffened composite panel using improved linear array", *Smart Struct. Syst.*, *Int. J.*, **24**(2), 173-182. https://doi.org/10.12989/sss.2019.24.2.173

HJ